

Doubly Protonated Benzene in the Gas Phase[†]Jana Roithová,^{*,‡,§} Detlef Schröder,^{*,‡} Robert Berger,[‡] and Helmut Schwarz[‡]

Institut für Chemie der Technischen Universität Berlin, Strasse des 17. Juni 135, D-10623 Berlin, Germany, J. Heyrovský Institute of Physical Chemistry, Academy of Sciences of the Czech Republic, Dolejškova 3, 182 23 Prague, Czech Republic, and FIAS, J.W. Goethe-University, Max-von-Laue-Strasse 1, D-60438 Frankfurt am Main, Germany

Received: August 3, 2005; In Final Form: October 20, 2005

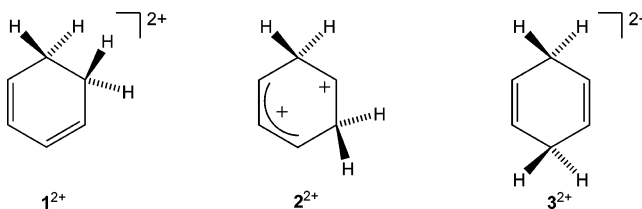
Structural aspects and the unimolecular fragmentations of doubly protonated benzene are studied by means of tandem-mass spectrometry. The corresponding dicationic species are generated by electron ionization (EI) of 1,3- and 1,4-cyclohexadienes, respectively. It is suggested that EI of 1,3-cyclohexadiene leads to the singlet state of doubly protonated benzene, whereas EI of 1,4-cyclohexadiene yields a mixture of singlet and triplet states. Unimolecular fragmentation of doubly protonated benzene exclusively proceeds via dehydrogenation leading to the benzene dication. The proton affinities (PAs) of protonated benzene amount to $PA(C_6H_7^+)_{meta} = 1.9 \pm 0.3$ eV for protonation taking place at the meta-position, $PA(C_6H_7^+)_{ortho} = 1.5 \pm 0.2$ eV, and $PA(C_6H_7^+)_{para} = 0.9 \pm 0.2$ eV, respectively. Various facets of the experiments are compared with density functional theory calculations and generally good agreement is found.

Introduction

Aspects of the structure and reactivity of protonated benzene, $C_6H_7^+$, continue to be of topical interest in physical organic chemistry and form still a subject of controversies.^{1,2} Nowadays, it is widely accepted that the structure of $C_6H_7^+$ corresponds to the so-called σ -complex in which one carbon atom of the ring has a sp^3 configuration. Detailed labeling experiments¹ revealed fast exchanges among the hydrogen atoms of $C_6H_7^+$ via a “ring-walk” mechanism³ and the absence of “memory effects” concerning the original position of the additional proton.^{1a,c,e} The proton affinity (PA) of neutral benzene amounts to $PA(C_6H_6) = 7.78$ eV.⁴

The existence of doubly protonated benzene, $C_6H_8^{2+}$, has been predicted by Sumathy and Kryachko using *ab initio* calculations at the MP2/6-311++G(d,p) level.⁵ Three constitutional isomers are conceivable with the additional proton in either ortho-, meta-, or para-position (1^{2+} , 2^{2+} , or 3^{2+} , respectively, Chart 1). According to these calculations, meta-diprotonated benzene, 2^{2+} , represents the most stable isomer with a geometry clearly corresponding to a σ -type complex in analogy to singly protonated benzene. The ortho-isomer 1^{2+} lies 0.21 eV higher in energy, and the bonding of protons is of prevailing σ -type with a certain amount of π -bonding. For the para-isomer 3^{2+} , two distinct minima exist: one corresponding to a σ -complex (0.71 eV above 2^{2+}) and another, more stable one, corresponding to a “ π -complex” of benzene with the protons bonded from opposite sides of the ring (0.61 eV above 2^{2+}). Nevertheless, the exothermic isomerization of either ortho- or para-isomer to the global minimum 2^{2+} is predicted to proceed via negligibly small energy barriers.⁵ Hence, rapid equilibration is to be expected. According to these calculations, the proton affinity

CHART 1



of singly protonated benzene at the meta-position amounts to 1.61 eV.⁵ Although there are experimental studies devoted to linear, conjugated $C_6H_8^{2+}$ dications,⁶ to the best of our knowledge no experimental investigation on doubly protonated benzene seems to have been reported.

Experimental and Computational Details

The experiments were performed with a modified VG ZAB/HF/AMD four-sector mass spectrometer of BEBE configuration (B stands for magnetic and E for electric sector), which has been described previously.⁷ Both, cations and dicationic species of interest were generated by electron ionization (70 eV) of appropriate neutral precursor molecules and accelerated by a potential of 8 kV.

Ionization energies of the corresponding monocations were determined in energy-resolved charge stripping (CS) experiments.⁸ By virtue of the superior energy resolution of E(1), energy-resolved CS was conducted with B(1)-only mass-selected precursor ions which were collided with oxygen (80% transmission, T) in the field-free region (FFR) between B(1) and E(1). Signals due to the mono- and dicationic species were recorded at energy resolutions $E/\Delta E \geq 4000$, and Q_{min} values were determined from the differences between the high-energy onsets of the mono- and the dication peaks.⁹ The kinetic energy scale was calibrated using CS of the molecular ion of toluene, $C_7H_8^+ \rightarrow C_7H_8^{2+}$, with $Q_{min}(C_7H_8^+) = 14.8 \pm 0.1$ eV¹⁰ using a multiplicative calibration scheme.¹¹ To determine the kinetic energy release (KER) associated with dehydrogenation, the corresponding

[†] Part of the special issue “William Hase Festschrift”.

* To whom correspondence should be addressed. E-mail: (J.R.) jana.roithova@jh-inst.cas.cz; (D.S.) Detlef.Schroeder@tu-berlin.de.

[‡] Institut für Chemie der Technischen Universität Berlin.

[§] Academy of Sciences of the Czech Republic.

[†] J. W. Goethe-University.

precursor ions $C_6H_8^{2+}$ were mass-selected by B(1) and fragmentations were monitored by E(1), and the KER was determined from the peak-width of the fragment ions $C_6H_6^{2+}$.

All other experiments were conducted with B(1)/E(1) mass-selected ions, thereby avoiding most of the interferences which are encountered when using two sectors only.¹² Fragmentations of metastable ions (MI) occurring in the field-free region preceding the second magnet (third FFR) were monitored by scanning B(2). The structures of the ions of interest were probed by collisional activation (CA) and charge-exchange (CE) spectra. To this end, the parent ions were collided with He (CA spectra, 80% T), O_2 (CE(O_2) spectra, 80% T), or Xe (CE(Xe) spectra, 80% T), and the fragmentations were monitored by scanning B(2). In addition, the $C_6H_6^{2+}$ daughter ions formed upon dehydrogenation of metastable $C_6H_8^{2+}$ were characterized by their CA and CE spectra (MI/CA and MI/CE, respectively). In these experiments, the parent dications $C_6H_8^{2+}$ were accelerated by a potential of 4 kV, mass-selected by means of B(1)/E(1), the $C_6H_6^{2+}$ ions formed from metastable $C_6H_8^{2+}$ in the 3rd FFR were mass-selected using B(2), and collided with either He (MI/CA spectra, 80% T) or O_2 (MI/CE spectra, 80% T) in the fourth field-free region between B(2) and E(2), while monitoring the ionic fragments by scanning the latter sector. For comparison, the CA and CE spectra of the dication generated from benzene were recorded as well. Here, $C_6H_6^{2+}$ was accelerated by a potential of 4 kV, mass-selected by means of B(1)/E(1)/B(2), and collided with He or O_2 in the fourth FFR. All spectra were accumulated with the AMD-Intectra data systems; 5–30 scans were averaged to improve the signal-to-noise ratios, and the final data were derived from two to seven independent measurements. For the determination of the relative abundances of H_2 -elimination from $C_6H_8^{2+}$, the naturally occurring dications containing one ^{13}C atom were investigated in order to avoid overlap with isobaric $C_3H_4^+$ monocations. In addition to the experiments described below, several alternative precursors of $C_6H_8^{2+}$ were investigated (e.g., di-*exo*-methylene cyclobutane, methylcyclopentadiene, and 1,3,5-hexatriene), to probe the possible formation of different ring sizes or acyclic compounds. As far as $C_6H_8^{2+}$ dications are concerned, the results were very similar to those described here, and moreover, none of these precursors could account for the observed differences between the dications generated from 1,3- and 1,4-cyclohexadiene, respectively. While we cannot strictly exclude the involvement of isomeric dication structures, none of these experimental findings has a clear implication to do so, and unless noted otherwise, we therefore restrict ourselves to the cyclohexadiene precursors.

All calculations were performed using the density functional hybrid method B3LYP¹³ in conjunction with the 6-311G(d,p) triple- ζ basis set as implemented in the Gaussian 98 suite.¹⁴ For all optimized structures, a frequency analysis at the same level of theory allows to assign them as genuine minima or transition structures as well as to calculate the zero-point vibrational energies (ZPVEs). Franck–Condon energies involved in vertical electron-transfer processes were estimated as the difference between the energy of the dication and the corresponding monocation with the geometry optimized for the dication. For comparison with the energetics determined experimentally, CCSD(T)/cc-pVTZ^{15,16} single-point calculations were performed for B3LYP/6-311G(d,p) optimized minima. Relative energies (E_{rel}) are given for 0 K, where the ZPVE was always calculated at the B3LYP level.

Using the B3LYP results, the lifetimes of the excited triplet states of $C_6H_8^{2+}$ dications $^31^{2+}$ and $^33^{2+}$, respectively, were

estimated. To this end, the density of states of $^12^{2+}$ and $^13^{2+}$ were computed at the energy of $^31^{2+}$ and $^33^{2+}$, respectively, using the harmonic B3LYP frequencies and then weighted by the respective Franck–Condon factors computed in the harmonic oscillator approximation as has been described previously in detail.¹⁷ The determination of the multidimensional Franck–Condon integrals takes the mode-mixing effects and geometrical changes into account.^{18,19} The thermal contributions were estimated from comparison of the Franck–Condon envelopes corresponding to vibrational Boltzmann distributions at 0, 298, and 400 K, respectively. The change of temperature leads only to small gradual increase of the Franck–Condon weighted density of states relevant for the transition from $^33^{2+}$ to $^13^{2+}$; therefore, only minor effects on the lifetime are anticipated.

Results and Discussion

Structure of Doubly Protonated Benzene. According to Sumathy and Kryachko,⁵ the meta-isomer 2^{2+} corresponds to the global minimum of the potential-energy surface (PES) of $C_6H_8^{2+}$. As a result of the negligible barriers (ca. 0.01 eV)⁵ associated with rearrangements of either the ortho- or para-isomer to the meta-form, it is expected that facile hydrogen rearrangements take place and thus an equilibrium among ortho-, meta-, and para-isomers of $C_6H_8^{2+}$ is established before any conceivable skeletal rearrangements or fragmentations can occur. Accordingly, the metastable ion (MI), collisional activation (CA), and charge-exchange (CE) spectra of mass-selected $C_6H_8^{2+}$ are expected to be identical when the dication is generated from either 1,3-cyclohexadiene (**1**) or 1,4-cyclohexadiene (**3**). The MI spectra of $C_6H_8^{2+}$ formed from **1** and **3** are indeed quite similar with loss of H_2 as the dominant process and all other fragmentations having negligible abundances. However, a more detailed analysis shows that the abundance of H_2 elimination relative to the parent ion is significantly larger for $C_6H_8^{2+}$ generated from **1** ($4.2 \pm 0.1\%$) than for $C_6H_8^{2+}$ produced from **3** ($3.6 \pm 0.1\%$). Similarly, the collisional activation spectra of $C_6H_8^{2+}$ are very close to each other (Figure 1a), except that the abundance of H_2 elimination are again different for dications $C_6H_8^{2+}$ generated from **1** and **3**, respectively (Table 1). The kinetic energy release (KER) associated with the unimolecular dehydrogenation amounts to about 10 meV for all $C_6H_8^{2+}$ ions investigated here. The negligible KER implies that dehydrogenation of the molecular dication occurs without barrier in excess of the reaction exothermicity. We note in passing that exploratory experiments using a multipole mass spectrometer²⁰ revealed that the benzene dication $C_6H_6^{2+}$ undergoes H/D exchange with D_2 to afford $C_6H_{6-n}D_n^{2+}$ ($n = 1-2$) products in ion/molecule reactions at quasi-thermal energies.²¹ This result further confirms that the dehydrogenation of $C_6H_8^{2+}$ occurs without reverse activation barrier.

Charge-exchange spectra with oxygen as collision gas (Table 1, Figure 1b shows the CE(O_2) spectrum of 3^{2+}) confirm these results and provide some additional information. Similar to the MI and CA spectra, the amount of H_2 elimination relative to the parent ion is slightly larger for $C_6H_8^{2+}$ generated from **1** than for $C_6H_8^{2+}$ produced from **3**. Another significant difference between the two spectra is found in the fragmentation patterns themselves. Thus, the CE(O_2) spectrum of $C_6H_8^{2+}$ generated from **3** shows more H^+ loss ($m/z = 79$) and less $C_6H_8^{+}$ ($m/z = 80$) in comparison to the CE(O_2) spectrum of $C_6H_8^{2+}$ generated from **1**. The ratio of $C_6H_8^{+}$: $C_6H_7^+$ is 1:2.4 for dications generated from **3**, whereas for dications generated from **1** this ratio amounts to 1:1.3.

Charge-exchange spectra with xenon as collision gas were recorded for comparison; Figure 1c shows the CE(Xe) spectrum

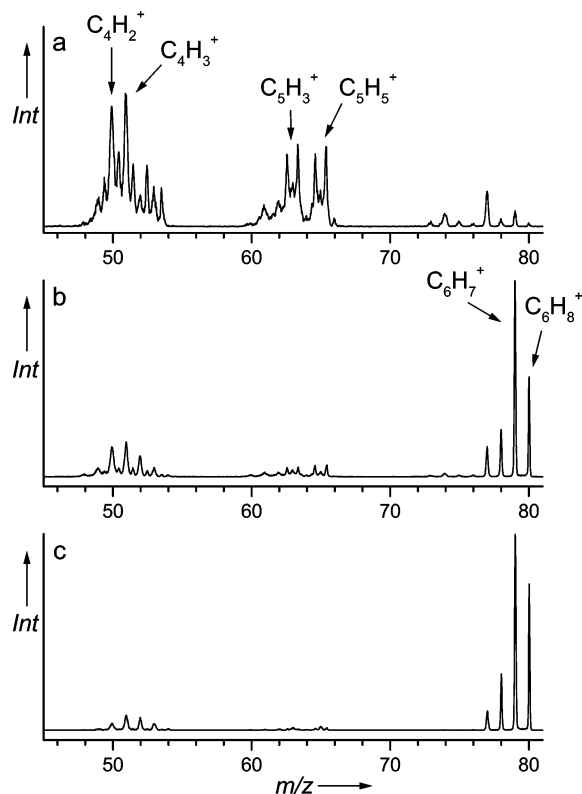


Figure 1. CA (a), CE(O₂) (b), and CE(Xe) (c) spectra of C₆H₈²⁺ dications generated upon EI of **3** (the spectra of C₆H₈²⁺ generated from **1** are given in the Supporting Information).

of **3**²⁺. Once more, the abundance of H₂ elimination is slightly more favored for C₆H₈²⁺ generated from **1** compared to C₆H₈²⁺ from **3**. Furthermore, the abundance of the C₆H₈⁺ signals and also the integrated intensities of all ions in the range *m/z* = 48–80 imply that charge exchange with xenon is more efficient for dications generated from **3**, whereas charge exchange with oxygen is slightly favored for C₆H₈²⁺ generated from **1**. The overall fragmentation patterns in the CE(Xe) spectra are quite similar to those in CE(O₂) spectra; only the C₆H_{*n*}⁺ ions are more abundant when xenon is used as collision gas. Similar to charge exchange with oxygen, the ratios of C₆H₈⁺:C₆H₇⁺ slightly differ for dications generated from **3** (1:1.8) and for those from **1** (1:1.3).

In summary, the experimental findings suggest that electron ionization of **1** and **3** does not lead to the same mixtures of isomers of doubly protonated benzene as is expected from the potential-energy surface of C₆H₈²⁺ reported by Sumathy and Kryachko.⁵ Specifically, the larger abundance of H₂ elimination for the dications generated from **1** could be ascribed to an ortho-effect,²² in that direct loss of H₂ would efficiently compete with a hydrogen ring-walk. However, such a scenario cannot explain the different abundances of H[•] elimination from the cations formed upon charge exchange of the dications, and it also does not account for the change in relative efficiencies of charge exchange in dependence on the nature of the collision gas (O₂ vs Xe). Thus, the existence of a more fundamental difference between the dication beams formed upon ionization of the different neutral precursors is indicated.

Complementary B3LYP calculations were performed aimed at understanding the origin of the different behavior of the C₆H₈²⁺ dications generated from **1** and **3**, respectively. In agreement with the previous MP2 study,⁵ the ortho-, meta-, and para-isomers of C₆H₈²⁺ were located as minima (Chart 1). However, a “ π -complex” which has been described for the para-

isomer **3**²⁺ represents only a shallow minimum at the B3LYP level, lying 0.02 eV higher in energy than the σ -complex **3**²⁺ of the para-isomer at the singlet ground state. As the B3LYP method cannot properly describe dispersion interactions,²³ which presumably play an important role in π -complexes, the geometry of the π -complex optimized at the MP2/6-311++G(d,p) level (as used in ref 5) has been adopted. Single-point calculations of all minima at the CCSD(T) level were then performed in order to achieve uniform energetics (values given in parentheses in Scheme 1). Accordingly, the π -complex represents a genuine minimum lying 0.15 eV lower in energy than the σ -complex. With respect to the negligible barrier (0.01 eV)⁵ found for the rearrangement of the π -complex of **1**²⁺ (singlet state of **3**²⁺) to the more stable isomer **1**²⁺, the para-isomer **1**³²⁺ is anyway considered as a fleeting species. In the following, the notation **1**³²⁺ refers to σ -complex found in the B3LYP calculations, and a discussion of the π -complex is not pursued any further.

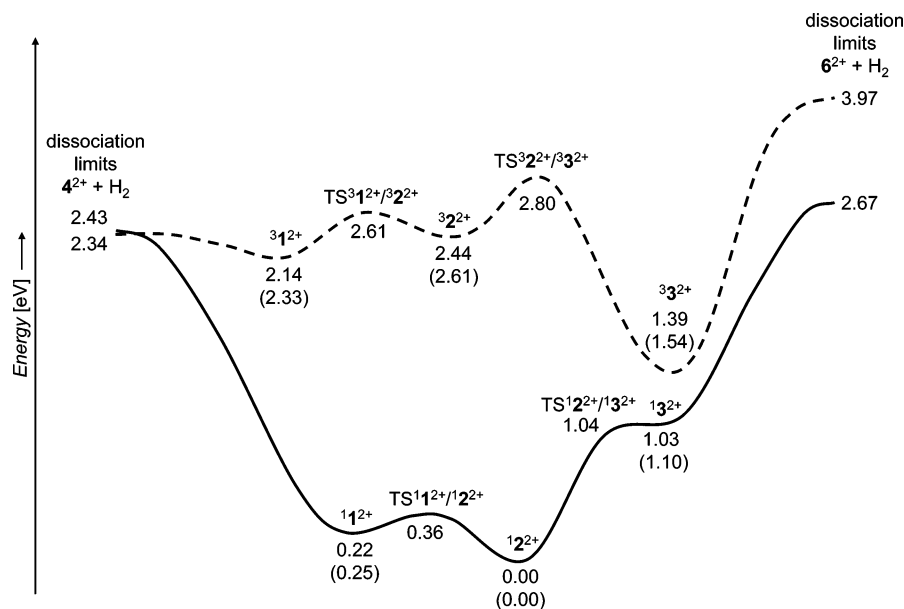
The calculated barriers for the hydrogen-ring walk in doubly protonated singlet benzene are very low indeed; i.e., 0.14 eV for **1**²⁺ → **1**²⁺ and 0.01 eV for **1**³²⁺ → **1**²⁺ (Scheme 1). In comparison, elimination of molecular hydrogen is a rather energy-demanding process. In the following, only dissociation limits for the elimination of a hydrogen molecule are considered. The corresponding transition structures are not determined, because the dominant interactions are generally described by the attractive potentials between the separating C₆H₆²⁺ dication and the neutral molecule H₂ which finally leads to rather loose transition structures typical for a continuously endothermic dissociation process.²⁴ This conclusion is also fully consistent with the lack of a reverse activation barrier of dehydrogenation as deduced from experiment (see above). The energetically lowest dissociation pathway corresponds to a 1,2-elimination of H₂ from ortho-diprotonated benzene **1**²⁺ and leads to the benzene dication **4**²⁺ in a “chairlike” conformation²⁵ (dissociation limit at *E*_{rel} = 2.43 eV, Scheme 1). We note in passing that the “pyramidal” skeleton of a C₅H₅ ring with a CH group at the apex was found to be the most stable isomer of singlet C₆H₆²⁺; it lies 0.06 eV lower in energy than **4**²⁺. The 1,1- and 1,2-eliminations of H₂ from the other isomers of singlet C₆H₈²⁺ lead to the energetically less favorable isomers **5**²⁺–**7**²⁺ of C₆H₆²⁺ (Chart 2) with the corresponding dissociation limits in an energy range of 2.7–2.8 eV (Table 2). Thus, the minimal energy required for H₂ elimination from C₆H₈²⁺ in the singlet state is more than 1 order of magnitude larger than the energy barriers associated with a hydrogen ring-walk. Consequently, complete equilibration among the isomers **1**²⁺, **1**²⁺, and **1**³²⁺ should be established prior to dehydrogenation.

These findings imply that double-ionization of **1** leads to a rather flat PES, in which the isomers **1**²⁺ and **1**²⁺ are preferentially populated (Scheme 1) and in which **1**²⁺ serves as an immediate precursor for the elimination of H₂. Likewise, ionization of **3** initially leads to **1**³²⁺, which is labile and undergoes prompt rearrangement, producing again a mixture of **1**²⁺ and **1**²⁺, but with a larger internal energy content. Thus, dehydrogenation of C₆H₈²⁺, produced from **3**, could be expected to be more pronounced than in the previous case. In marked contrast, however, the experimental results provide evidence that H₂ elimination is slightly favored for C₆H₈²⁺ generated from **1** rather than **3**. This contradiction holds true even if possible skeletal rearrangements of C₆H₈²⁺ are considered. Thus, primarily the equilibrium among **1**²⁺, **1**²⁺, and **1**³²⁺ is established, and in the second step, more energy-demanding C–C bond cleavages can occur. For example, the most stable open-chain dication C₆H₈²⁺ derived from 1,3,5-hexatriene (*E*_{rel} = 0.34 eV)

TABLE 1: MI, CA, and CE Spectra^{a,b} of Dications C₆H₈²⁺ Generated from 1,3-Cyclohexadiene (**1**) and 1,4-Cyclohexadiene (**3**)

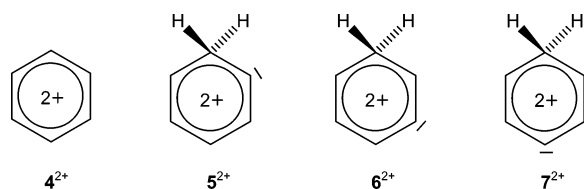
<i>m/z</i>	fragment ion	MI		CA		CE(O ₂)		CE(Xe)	
		1	3	1	3	1	3	1	3
39	C ₆ H ₆ ²⁺	4.2	3.6	4.6	4.2	4.5	4.0	4.3	4.1
48–54	C ₄ H _{<i>n</i>}			10 × 10 ²	10 × 10 ²	18 × 10 ²	18 × 10 ²	20 × 10 ²	24 × 10 ²
60–66	C ₃ H _{<i>n</i>}			7 × 10 ²	7 × 10 ²	8 × 10 ²	9 × 10 ²	6 × 10 ²	8 × 10 ²
77	C ₆ H ₅ ⁺			0.6 × 10 ²	0.4 × 10 ²	3 × 10 ²	2 × 10 ²	5 × 10 ²	6 × 10 ²
78	C ₆ H ₆ ⁺			0.1 × 10 ²	<0.1 × 10 ²	3 × 10 ²	2 × 10 ²	8 × 10 ²	8 × 10 ²
79	C ₆ H ₇ ⁺			0.2 × 10 ²	0.2 × 10 ²	11 × 10 ²	12 × 10 ²	30 × 10 ²	42 × 10 ²
80	C ₆ H ₈ ⁺			<0.1 × 10 ²	<0.1 × 10 ²	8 × 10 ²	5 × 10 ²	23 × 10 ²	24 × 10 ²
48–80	C ₄ H _{<i>n</i>} –C ₆ H _{<i>n</i>}			18 × 10 ²	18 × 10 ²	51 × 10 ²	48 × 10 ²	92 × 10 ²	112 × 10 ²

^a The intensities are derived from integrated peak areas relative to the area of the peak corresponding to the parent dication C₆H₈²⁺, which was set to 100. ^b The naturally occurring dications C₆H₈²⁺ with one ¹³C atom were investigated in order to avoid overlap with isobaric C₃H₄⁺ monocations.

SCHEME 1. Schematic PES of Singlet (Solid Line) and Triplet (Dashed Line) C₆H₈²⁺ Isomers Calculated at the B3LYP Level^a

^a Energies are given in eV at 0 K, relative to the most stable isomer ¹2⁺ ($E_{\text{tot}} = -232.688775$ hartree, ZPVE = 0.117076 hartree). Energies in brackets are derived from single-point calculations performed at the CCSD(T) level. For the energetics and structural representations of ⁴2⁺–⁷2⁺, see Table 2 and Chart 2.

CHART 2

TABLE 2: B3LYP/6-311G(d,p) Energies at 0 K of C₆H₆²⁺ + H₂ Dissociation Limits of C₆H₈²⁺ Leading to Doubly Ionized Benzene (⁴2⁺) and Some of Its Proton-Shift Isomers (⁵2⁺–⁷2⁺)^a

state	$E_{\text{rel}}(\text{C}_6\text{H}_6^{2+} + \text{H}_2)$ [eV]			
	⁴ 2 ⁺ + H ₂	⁵ 2 ⁺ + H ₂	⁶ 2 ⁺ + H ₂	⁷ 2 ⁺ + H ₂
singlet	2.43	2.80	2.67	2.75
triplet	2.34	3.93	3.97	4.03

^a Energies are given relative to ¹2⁺.

can be achieved from the ortho-isomer ¹1²⁺. The energy barrier associated with this process amounts to $E_{\text{rel}} = 1.05$ eV. Hence, the number of accessible C₆H₈²⁺ isomers can be accordingly larger. Nevertheless, the expected trend for dehydrogenation does not change in quality: The fragmentation of metastable dications C₆H₈²⁺ generated either from **1** or **3** should be the

same, or the dications generated from **3** should reflect the higher internal energy content. In this context, we further note in passing that the metastable ion spectra of the C₆H₈²⁺ dications generated from 1,3,5-hexatriene show again dehydrogenation as exclusive fragmentation, but its abundance (3% relative to the parent dications) is lower than that found for the dications C₆H₈²⁺ generated either from **1** or **3** (Table 1).

As a possible explanation for the differences in the fragmentation patterns of the C₆H₈²⁺ ions formed upon EI of **1** and **3**, respectively, the direct generation of the excited triplet states ³1²⁺ and ³3²⁺ is considered. Many factors influence the relative efficiencies of the formation and the stabilities of the triplet states vs the singlet-ground states. For their formation by electron ionization, the associated Franck–Condon factors play an important role. An idea about the corresponding efficiencies can be achieved from the differences between vertical and adiabatic ionization energies ($\Delta E_{\text{v/a}}$).

The triplet ³1²⁺ lies 1.92 eV higher in energy than the singlet ground state of this isomer (Scheme 1). Its formation is associated with $\Delta E_{\text{v/a}}(1^3\text{1}^{2+}) = 0.46$ eV. The energy required for 1,2-dehydrogenation of ³1²⁺ to yield the triplet state of the benzene dication ³4²⁺ ($E_{\text{rel}} = 2.34$ eV) amounts only to 0.20 eV. This situation suggests that the triplet dication ³1²⁺, if formed at all, undergoes immediate loss of a hydrogen molecule.

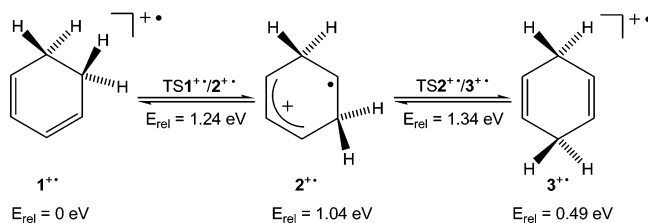
As to the probability to form both singlet and triplet ortho-diprotonated benzene, the formation of 1^{2+} is associated with a lower $\Delta E_{v/a}(1^{12+}) = 0.29$ eV than the formation of 3^{12+} ($\Delta E_{v/a}(3^{12+}) = 0.46$ eV); therefore, also Franck–Condon factors most probably favor the formation of the singlet ground state. On the other hand, the energy difference between 1^{32+} and 3^{32+} amounts to only 0.36 eV. The formation of the triplet state is associated with a lower $\Delta E_{v/a}(3^{32+}) = 0.16$ eV than the formation of the singlet state; the latter if formed with $\Delta E_{v/a}(3^{132+}) = 0.28$ eV. Thus, it is quite likely that also the triplet state is formed upon electron ionization of **3**. Similarly to 3^{12+} , the lifetime of the excited triplet state 3^{32+} can be affected by dehydrogenation. The lowest dissociation limit leading to the triplet state of benzene dication ($E_{\text{rel}} = 2.34$ eV) can be achieved only upon a series of rearrangements (Scheme 1). Nonetheless, the rearrangement of 3^{32+} ($E_{\text{rel}} = 1.39$ eV) to the other isomers of doubly protonated benzene is prevented by an appreciable barrier ($\text{TS}^{32+/3^{32+}}$, $E_{\text{rel}} = 2.80$ eV) and also isomers 3^{12+} and 3^{32+} themselves are rather high in energy ($E_{\text{rel}} = 2.14$ and 2.44 eV, respectively). The direct dehydrogenation of 3^{32+} leads to one of the less stable isomers of $\text{C}_6\text{H}_6^{2+}$ (Chart 2): A 1,1-dehydrogenation leads to 3^{72+} ($E_{\text{rel}} = 4.03$ eV), and a 1,2-dehydrogenation yields the isomer 3^{62+} ($E_{\text{rel}} = 3.97$ eV). Accordingly, a lowered yield of dehydrogenation is expected for 3^{32+} .

The lifetimes of the excited states further depend on the propensity for radiation-less transitions to the respective spin ground states.²⁶ The efficiency of the spin-isomerization process for the transition $3^{32+} \rightarrow 1^{32+}$ is estimated on the basis of an analysis of the spin–orbit coupling elements H_{SO} . The symmetries of the wave function for 1^{32+} (1A_1) and 3^{32+} ($^3B_{2u}$) are different which results in vanishing of the zeroth order spin–orbit coupling element $H_{\text{SO}}^{(0)}$. Thus, only oscillations from the equilibrium structure can contribute to H_{SO} . Accordingly, the first-order spin–orbit coupling element $H_{\text{SO}}^{(1)}$ was roughly estimated using an approximation of the analytical derivative by small changes of the equilibrium geometry of 3^{32+} . This approach leads to a value of $H_{\text{SO}}^{(1)} \approx 0.0002$ cm⁻¹, which corresponds to an estimate of the lifetime of 3^{32+} in the ground vibrational state in the order of microseconds. Without further arguing about the accuracy of this estimate, we suggest that a significant population of 3^{32+} might be present in the mass-selected $\text{C}_6\text{H}_8^{2+}$ beam obtained upon electron ionization of **3**. We note in passing that for the ortho-isomer 3^{12+} , the direct coupling is not symmetry forbidden, which results in value of $H_{\text{SO}} \approx 0.3$ cm⁻¹, and thus its lifetime is much shorter than that of 3^{32+} .

Within this framework, a straightforward rationale can be put forward for the experimental results. Electron ionization of **1** leads preferentially, if not exclusively, to the singlet surface of doubly protonated benzene, whereas EI of **3** provides access to singlet as well as triplet states. Given that dehydrogenation of $\text{C}_6\text{H}_8^{2+}$ is easier to achieve on the singlet surface, any significant population of triplet $\text{C}_6\text{H}_8^{2+}$ to the beam of mass-selected dications decreases the relative abundance of H_2 elimination. Accordingly, this scenario can account for the lower amount of dehydrogenation for the dications generated from **3**.

The charge-exchange experiments lend further support to the proposed differences in the population of singlet and triplet states in the $\text{C}_6\text{H}_8^{2+}$ ion beams generated from neutral **1** and **3**, respectively. Charge exchange in keV-collisions can be considered to occur as a vertical process and as such is governed by Franck–Condon factors. The efficiency of such a transition and also the amount of associated internal excitation can be

SCHEME 2. B3LYP Relative Energies of Three Isomers of $\text{C}_6\text{H}_8^{2+}$ and Barriers for Their Interconversion^a



^a Energies are given at 0 K relative to the most stable isomer 1^{2+} ($E_{\text{tot.}} = -233.193506$ hartree, ZPVE = 0.120844 hartree).

roughly estimated from the difference between vertical and adiabatic energies of the charge-exchange process ($\Delta E_{v/a}$). As detailed above, the singlet dications are expected to be mostly populated as the ortho- and meta-isomers, 1^{12+} and 1^{22+} . Charge exchange of 1^{22+} is associated with a substantial internal excitation of $\Delta E_{v/a}(1^{22+}/1^{2+}) = 1.11$ eV, which suggests that the transition is associated with unfavorable Franck–Condon factors. Hence, low efficiency and extensive fragmentation of the resulting $\text{C}_6\text{H}_8^{2+}$ monocation is expected in the charge exchange of 1^{22+} . In contrast, charge exchange of 1^{12+} is associated with a $\Delta E_{v/a}(1^{12+}/1^{1+})$ of only 0.28 eV and leads to the more stable isomer of $\text{C}_6\text{H}_8^{2+}$ (Scheme 2). Hence, in a mixture of 1^{12+} and 1^{22+} , mainly the ortho-isomer 1^{12+} is expected to undergo charge exchange. On the triplet surface, only 3^{32+} is likely to be formed in considerable amounts (see above). Charge exchange of 3^{32+} is associated with a small additional internal excitation of $\Delta E_{v/a}(3^{32+}/3^{3+}) = 0.16$ eV and leads to the para-isomer 3^{3+} which is 0.5 eV higher in energy than 1^{1+} . Thus, the energy required for H^\bullet elimination from 3^{3+} to produce singly protonated benzene is lower than for 1^{1+} which can explain the difference in relative abundance of H^\bullet elimination in CE spectra of dications generated from **1** and **3**.

The relative increase of the CE cross section for the $\text{C}_6\text{H}_8^{2+}$ dications generated from **3** upon changing the collision gas from O_2 to Xe, compared to dications generated from **1**, can also be explained by the presence of 3^{32+} . The ground state of oxygen is a triplet. On the basis of spin-conservation rules, all couplings of the singlet dication with $^3\text{O}_2$ should lead to the ground states of products, whereas the triplet dication may also lead to the formation of $\text{C}_6\text{H}_8^{2+}$ in excited quartet states, which can cause a lower overall cross section of charge exchange. In comparison, charge exchange with xenon in its ground state should lead to the ground-state products for all couplings with both, singlet and triplet states of the dication. Accordingly, the cross section for charge exchange of 3^{32+} increases upon change of O_2 by Xe as collision gas. Note, however, that other factors like exothermicity of the charge exchange for different isomers and states may also play a role.

Fragmentation of Doubly Protonated Benzene. The by far most important process in the fragmentation of $\text{C}_6\text{H}_8^{2+}$ corresponds to the loss of molecular hydrogen. For the interpretation of the fragmentation pattern, it is important to identify which signals originate from subsequent decomposition of $\text{C}_6\text{H}_6^{2+}$ formed by unimolecular fragmentation of metastable $\text{C}_6\text{H}_8^{2+}$. To resolve this problem, MI/CA and MI/CE spectra of $[\text{C}_6\text{H}_8^{2+} - \text{H}_2]$ have been recorded. As expected,²⁷ the MI/CA and also the MI/CE spectra of $[\text{C}_6\text{H}_8^{2+} - \text{H}_2]$ generated from **1** and **3** are identical; Figure 2 shows the MI/CA and the MI/CE spectra of $[\text{C}_6\text{H}_8^{2+} - \text{H}_2]$ generated from **3**. We further note that the MI/CA and MI/CE spectra are identical with the CA and CE spectra of the dication $\text{C}_6\text{H}_6^{2+}$ generated directly by EI of benzene (see Supporting Information). The major process in

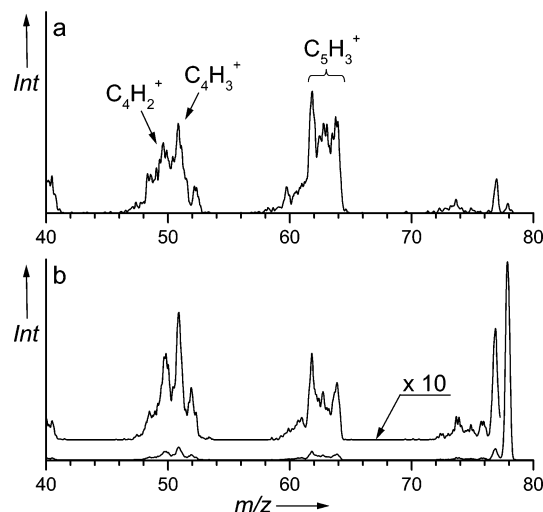
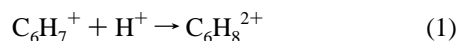


Figure 2. High-mass regions of the MI/CA (a) and MI/CE (b) spectra of the daughter ion $C_6H_6^{2+}$ arising from metastable $C_6H_8^{2+}$ generated from **3** (MI/CA and MI/CE spectra of $[C_6H_8^{2+} - H_2]$ generated from **1** and also CA and CE spectra of $C_6H_6^{2+}$ generated from benzene can be found in the Supporting Information).

fragmentation of $C_6H_6^{2+}$ corresponds to the elimination of the CH_3^+ cation concomitant with a $C_5H_3^+$ fragment ($m/z = 63$). The composite shape of the corresponding peak is a result of the Coulomb explosion of the dications into two singly charged ions.²⁸ Other fragmentations originate from losses of C_2 -fragments upon charge exchange, among which the dominant processes lead to $C_4H_3^+$ ($m/z = 51$) and $C_4H_2^+$ ($m/z = 50$).

With regard to the fragmentation of doubly protonated benzene (Figure 1), two dominant composite peaks can be seen among the peaks corresponding to C_1 -losses. One originates from the elimination of a methyl cation ($m/z = 65$) and the other one ($m/z = 63$) comes most probably from a two-step fragmentation. In the first step, a neutral hydrogen molecule is eliminated which is then followed by the expulsion of a methyl cation (see above). Signals associated with C_2 -eliminations originate preferentially from the fragmentation of the parent ion upon charge exchange. The two dominant processes are due to the losses of $[C_2, H_6]$ ($m/z = 50$) and $[C_2, H_5]^+$ ($m/z = 51$) which, again, most probably represent sequential fragmentations: First, a molecule of hydrogen is eliminated and in the second step the C–C bond cleavage occurs; this is well reflected in the MI/CA and MI/CE spectra of $[C_6H_8^{2+} - H_2]$ (Figure 2). The same fragmentations can also occur prior to H_2 elimination which is indicated by the signals at $m/z = 52$ and 53 . In summary, the major channel in the fragmentation of doubly protonated benzene leads to the benzene dication. Other fragmentation channels probably follow pathways similar to those found for the benzene dication.^{29,30}

Proton Affinity of Protonated Benzene. The proton affinity of $C_6H_7^+$ corresponds to the enthalpy of reaction 1.



with $PA = -\Delta_f H$

The obvious difficulties associated with a direct determination of the exothermicity of a reaction involving two cations are usually circumvented by means of thermochemical cycles. This approach consists of independent determinations of $\Delta_f H$ of the corresponding cation and dication in conjunction with $\Delta_f H(H^+) = 15.86$ eV at 298 K.^{31,32} Thus, $\Delta_f H$ of $C_6H_7^+$ can be determined from $\Delta_f H(C_6H_6) = 0.86 \pm 0.01$ eV,³³ and the proton

TABLE 3: MI and CA Spectra^a of $C_6H_8^{+}$ Generated from 1,3-Cyclohexadiene (1**) and 1,4-Cyclohexadiene (**3**)**

m/z	fragment ion	MI		CA	
		1 ⁺	3 ⁺	1 ⁺	3 ⁺
77	$C_6H_5^+$	0.1	0.8	10	27
78	$C_6H_6^{+}$	7	15	12	19
79	$C_6H_7^+$	100	100	100	100

^a The intensities are derived from integrated peak areas relative to the area of the peak corresponding to $C_6H_7^+$ fragment which was set to 100.

affinity $PA(C_6H_6) = 7.78$ eV^{4b} which leads to $\Delta_f H(C_6H_7^+) = 8.94 \pm 0.01$ eV.

A direct experimental determination of $\Delta_f H(C_6H_8^{2+})$ requires the knowledge of $\Delta_f H$ of the neutral precursor C_6H_8 and its first and second ionization energies. In the present case, however, this seemingly straightforward approach is complicated by two factors. The first problem arises from the structure of the neutral precursor C_6H_8 , because only 1,3- and 1,4-cyclohexadiene are available which serve as precursors for the ortho- and para-isomers of $C_6H_8^{2+}$, whereas the most stable isomer of doubly protonated benzene corresponds to m - $C_6H_8^{2+}$. We note in passing that attempts to generate m - $C_6H_8^{2+}$ by dissociative EI of 3,5-dichlorocyclohexene failed due to insufficient yields of the desired fragment ions. Therefore, the proton affinity for protonation at the meta-position of $C_6H_8^{2+}$ is determined indirectly from the experimental values derived for the proton affinities at the ortho- and para-positions and the calculated relative stabilities of **1**²⁺, **2**²⁺, and **3**²⁺. The method of choice for the determination of the second ionization energies of **1** and **3**, respectively, is charge-stripping (CS).⁸ Such experiments are based on the formation and mass-selection of the corresponding singly charged cation (**1**⁺ and **3**⁺, respectively), followed by further ionization in a collision with a suitable target gas (usually oxygen).^{8,10} The energy required for ionization is taken from the kinetic energy of the projectile monocation and can be determined in energy-resolved measurements. While the precision of CS experiments is limited to a few tenths of an eV,⁹ the key advantage of CS is its applicability to mass-selected ion beams. It needs to be pointed out, however, that ascribing the ionization energy of a cation determined by the CS method to the second ionization energy of the corresponding neutral molecule requires that the connectivity of the cation corresponds to the connectivity of the neutral. This leads to yet a further uncertainty in the case of C_6H_8 , because cations of hydrocarbons are well-known to undergo facile isomerizations.^{3,34} Accordingly, it cannot be taken for granted that $C_6H_8^{+}$ monocations keep the structures of their corresponding neutral precursors.

Qualitative information about the structures of the $C_6H_8^{+}$ cations generated from **1** and **3** can be derived from their metastable ion (MI) and collisional activation (CA) spectra (Table 3). All spectra are dominated by losses of atomic hydrogen which leads to the formation of protonated benzene. In addition, the MI spectra contain two minor peaks, which correspond to eliminations of H_2 and $[H_3]^+$, respectively; the latter most likely corresponds to consecutive elimination of H^+ and H_2 . Both processes are relatively more abundant for **3**⁺ than for **1**⁺. The CA spectra show a similar trend. Cation **3**⁺ again provides more abundant losses of H_2 and $[H_3]^+$, and the latter is even more abundant than the elimination of H_2 . These results suggest a significant difference between the cations generated upon EI of **1** and **3**. Thus, an equilibrium between **1**⁺ and **3**⁺ (and optionally other $C_6H_8^{+}$ isomers) is apparently not reached.

TABLE 4: Experimentally and Theoretically^a Determined Ionization Energies and Proton Affinities (in eV)

	IE _{exp}	IE _{calc}	ΔIE _{v/a}
1 ⁺	14.0 ± 0.2	13.79	0.28
3 ⁺	14.0 ± 0.2	14.07 (13.92) ^b	0.23 (0.37) ^b
	PA(C ₆ H ₇ ⁺) _{ortho}	PA(C ₆ H ₇ ⁺) _{meta}	PA(C ₆ H ₇ ⁺) _{para}
experimental value	1.5 ± 0.2	1.9 ^c ± 0.3	0.9 ± 0.2
theoretical value ^d	1.59	1.84	0.74 (0.89) ^c
theoretical value ^e	1.40	1.61	0.90 (1.00)

^a Values were derived from CCSD(T)/cc-pVTZ single point energies of minima optimized at B3LYP/6-311G(d,p) level. ^b Values in parentheses correspond to ionization to the “π-complex”. Its geometry was optimized at the MP2/6-311++G(2d,p) level. ^c The value is determined from a combination of experimentally determined proton affinities at the ortho- and para-positions and the calculated relative energies of 1²⁺, 2²⁺, and 3²⁺ (see also text). ^d This work. ^e Reference 6.

In agreement with these experimental findings, B3LYP calculations (Scheme 2) predict that both isomers are separated by a considerable barrier exceeding 1 eV. Already the meta-isomer 2⁺, which serves as an intermediate between the two cations discussed, lies 1.04 eV higher in energy than 1⁺. Thus, it appears justified to suppose that at least part of the cations C₆H₈¹⁺ generated either from 1 or from 3 keep the connectivities of their neutral precursors. Accordingly, charge-stripping appears as a reasonable approach for the determination of the second ionization energies of 1 and 3.

Within this framework, Δ_fH(1²⁺) results from the heat of formation of 1,3-cyclohexadiene Δ_fH(1) = 1.08 ± 0.01 eV,³⁵ its first ionization energy IE(1) = 8.25 ± 0.02 eV,³⁶ and the second ionization energy IE(1⁺) = 14.0 ± 0.2 eV as determined by CS. The summation leads to Δ_fH(1²⁺) = 23.3 ± 0.2 eV. Accordingly, the proton affinity of C₆H₇⁺ for protonation at the ortho-position evolves as PA(C₆H₇⁺)_{ortho} = 1.5 ± 0.2 eV. Similarly, the proton affinity for the protonation at the para-position can be determined from Δ_fH(3) = 1.04 ± 0.03 eV,³⁷ IE(3) = 8.82 eV³⁶ and IE(3⁺) = 14.0 ± 0.2 eV, which lead to a value of PA(C₆H₇⁺)_{para} = 0.9 ± 0.2 eV.

For comparison, the corresponding ionization energies are also available from theory (Table 4). CCSD(T)/B3LYP calculations lead to values of IE_{calc}(1) = 8.17 eV and IE_{calc}(3) = 8.74 eV, which is in good agreement with the experimental data (8.25 and 8.82 eV, respectively)³⁶ and demonstrates the accuracy of the method. The second ionization energies amount to IE_{calc}(1⁺) = 13.79 eV and IE_{calc}(3⁺) = 14.07 eV.³⁸ Thus, the theoretical values agree very well with the ionization energies determined by CS with the deviation being larger for the ortho-isomer. The difference between vertical and adiabatic ionization energies (ΔIE_{v/a}) are relatively small (ΔIE_{v/a}(1⁺/1²⁺) = 0.28 eV and ΔIE_{v/a}(3⁺/3²⁺) = 0.23 eV), which suggests that the values derived from CS experiments correspond to adiabatic rather than vertical IEs.¹⁰

On the basis of all results, the proton affinity of C₆H₇⁺ for protonation at the meta-position can finally be determined. Within the CCSD(T)/B3LYP theoretical approach, 1²⁺ and 3²⁺ lie 0.25 and 1.10 eV, respectively, higher in energy than the most stable meta-isomer 2²⁺ (Scheme 1). Relative to the ortho-isomer, the proton affinity of C₆H₇⁺ for protonation at the meta-position can hence be determined as 1.8 ± 0.3 eV. Likewise, the results obtained for para-protonation provide the proton affinity of C₆H₇⁺ for protonation at the meta-position of 2.0 eV ± 0.2. The average of 1.9 ± 0.3 eV is thus considered as the best estimate for PA(C₆H₇⁺)_{meta}.

Conclusions

Electron ionization of 1,3-cyclohexadiene (1) generates predominantly, if not exclusively, the singlet state of doubly protonated benzene, whereas the formation of a mixture of singlet and triplet states can best account for the behavior of the C₆H₈²⁺ ions formed upon EI of 1,4-cyclohexadiene (3). Specifically, it is suggested that the *p*-C₆H₈²⁺ isomer can exist as a triplet state which has a sufficient lifetime (in the order of microseconds) to allow for mass spectrometric investigations.³⁹ The major fragmentation reaction of doubly protonated benzene corresponds to dehydrogenation which leads to the formation of a benzene dication; the reaction takes place on the singlet potential-energy surface.

Interestingly, the proton affinity of protonated benzene is still positive. The experimentally determined proton affinities amount to PA(C₆H₇⁺)_{ortho} = 1.5 ± 0.2 eV and PA(C₆H₇⁺)_{para} = 0.9 ± 0.2 eV. Combination of these values with calculated energy differences between the ortho-, meta-, and para-isomers of doubly protonated benzene provides a value of PA(C₆H₇⁺)_{meta} = 1.9 ± 0.3 eV.

Acknowledgment. Continuous financial support by the European Commission (MCInet), the Deutsche Forschungsgemeinschaft, the Fonds der Chemischen Industrie, and the Gesellschaft von Freunden der Technischen Universität Berlin is gratefully acknowledged. J.R. is grateful for the support of the Grant Agency of the Academy of Sciences of the Czech Republic (No. KJB4040302). R.B. acknowledges financial support by the Volkswagen foundation.

Supporting Information Available: The CA, CE(O₂), and CE(Xe) spectra of C₆H₈²⁺ generated from 1 (Figure S1), the MI/CA and MI/CE spectra of [C₆H₈²⁺-H₂] generated from 1 (Figure S2), and the CA and CE spectra of C₆H₆²⁺ generated from benzene (Figure S3). This material is available free of charge via the Internet at <http://pubs.acs.org>.

References and Notes

- (1) (a) Kuck, D.; Schneider, J.; Grützmacher, H.-Fr. *J. Chem. Soc., Perkin Trans. 2* **1985**, 689. (b) DePuy, C. H.; Gareyev, R.; Fornarini, S. *Int. J. Mass Spectrom. Ion Processes* **1997**, *161*, 41. (c) Mormann, M.; Kuck, D. *Int. J. Mass Spectrom.* **2002**, *219*, 497. (d) Ascenzi, D.; Bassi, D.; Franceschi, P.; Tosi, P.; Di Stefano, M.; Rosi, M.; Sgamellotti, A. *J. Chem. Phys.* **2003**, *119*, 8366. (e) Schröder, D.; Loos, L.; Schwarz, H.; Thissen, R.; Dutuit, O. *J. Phys. Chem. A*, **2004**, *108*, 9931.
- (2) (a) Kuck, D. *Mass Spectrom. Rev.* **1990**, *9*, 583. (b) Glukhovtsev, M. N.; Pross, A.; Nicolaidis, A.; Radom, L. *J. Chem. Soc. Chem. Commun.* **1995**, 2347. (c) Mason, R. S.; Williams, C. M.; Anderson, P. D. *J. J. Chem. Soc., Chem. Commun.* **1995**, 1027.
- (3) Kuck, D. *Int. J. Mass Spectrom.* **2002**, *213*, 101.
- (4) (a) Szulejko, J. E.; McMahon, T. B. *J. Am. Chem. Soc.* **1993**, *115*, 7839. (b) Hunter, E. P.; Lias, S. G. *J. Phys. Chem. Ref. Data* **1998**, *27*, 413.
- (5) Sumathy, R.; Kryachko, E. S. *J. Phys. Chem. A* **2002**, *106*, 510.
- (6) (a) Jones, B. E.; Abbey, L. E.; Chatham, H. L.; Hanner, A. W.; Teleshefsky, L. A.; Burgess, E. M.; Moran, T. F. *Org. Mass Spectrom.* **1982**, *17*, 10. (b) Radhakrishnan, T. P.; Agranat, I. *J. Org. Chem.* **2001**, *66*, 3215.
- (7) Schalley, C. A.; Schröder, D.; Schwarz, H. *Int. J. Mass Spectrom. Ion Processes* **1996**, *153*, 173.
- (8) Cooks, R. G.; Beynon, J. H.; Litton, J. F. *Org. Mass Spectrom.* **1975**, *10*, 503 and references therein.
- (9) McCullough-Catalano, S.; Lebrilla, C. B. *J. Am. Chem. Soc.* **1993**, *115*, 1441.
- (10) Roithová, J.; Schröder, D.; Loos, J.; Schwarz, H.; Jankowiak, H.-C.; Berger, R.; Thissen, R.; Dutuit, O. *J. Chem. Phys.* **2005**, *122*, 094306.
- (11) Lammertsma, K.; Schleyer, P. v. R.; Schwarz, H. *Angew. Chem.* **1989**, *101*, 1313; *Angew. Chem., Int. Ed. Engl.* **1989**, *28*, 1321.
- (12) Schröder, D.; Schwarz, H. *Int. J. Mass Spectrom.* **1995**, *146/147*, 183.

- (13) (a) Vosko, S. H.; Wilk, L.; Nusair, M. *Can. J. Phys. (Paris)*. **1980**, 58, 1200. (b) Lee, C.; Yang, W.; Parr, R. G. *Phys. Rev. B* **1988**, 37, 785. (c) Miehllich, B.; Savin, A.; Stoll, H.; Preuss, H. *Chem. Phys. Lett.* **1989**, 157, 200. (d) Becke, A. D. *J. Chem. Phys.* **1993**, 98, 5648.
- (14) Frisch, M. J.; Trucks, G. W.; Schlegel, H. B.; Scuseria, G. E.; Robb, M. A.; Cheeseman, J. R.; Zakrzewski, V. G.; Montgomery, J. A.; Stratmann, R. E.; Burant, J. C.; Dapprich, S.; Millam, J. M.; Daniels, A. D.; Kudin, K. N.; Strain, M. C.; Farkas, O.; Tomasi, J.; Barone, V.; Cossi, M.; Cammi, R.; Mennucci, B.; Pomelli, C.; Adamo, C.; Clifford, S.; Ochterski, J.; Petersson, G. A.; Ayala, P. Y.; Cui, Q.; Morokuma, K.; Malick, D. K.; Rabuck, A. D.; Raghavachari, K.; Foresman, J. B.; Cioslowski, J.; Ortiz, J. V.; Baboul, A. G.; Stefanov, B. B.; Liu, G.; Liashenko, A.; Piskorz, P.; Komaromi, I.; Gomperts, R.; Martin, R. L.; Fox, D. J.; Keith, T.; Al-Laham, M. A.; Peng, C. Y.; Nanayakkara, A.; Gonzalez, C.; Challacombe, M.; Gill, P. M. W.; Johnson, B. G.; Chen, W.; Wong, M. W.; Andres, J. L.; Head-Gordon, M.; Replogle, E. S.; Pople, J. A. *Gaussian 98*, revision A.11. Gaussian, Inc.: Pittsburgh, PA, 1998.
- (15) Čížek, J. *Adv. Chem. Phys.* **1969**, 14, 35.
- (16) Kendall, R. A.; Dunning, T. H., Jr.; Harrison, R. J. *J. Chem. Phys.* **1992**, 96, 6796.
- (17) (a) Berger, R.; Klessinger, M. *J. Comput. Chem.* **1997**, 18, 1312. (b) Berger, R.; Fischer, C.; Klessinger, M. *J. Phys. Chem. A* **1998**, 102, 7157.
- (18) Doktorov, E.; Malkin, I.; Man'ko, V. *J. Mol. Spectrosc.* **1977**, 56, 1.
- (19) Dushinsky, F. *Acta Physicochim. URSS* **1937**, 7, 551.
- (20) Roithová, J.; Schröder, D.; Grüne, P.; Weiske, T.; Schwarz, H. *J. Phys. Chem.*, in press.
- (21) Roithová, J.; Herman, Z.; Schröder, D.; T.; Schwarz, H. Unpublished results.
- (22) Schwarz, H. *Top. Curr. Chem.* **1978**, 73, 231.
- (23) Rappé, A. K.; Bernstein, E. R. *J. Phys. Chem. A* **2000**, 104, 6117.
- (24) For computational details of the closely related H₂ loss from C₆H₇⁺, see: Bouchoux, G.; Yáñez, M.; Mó, O. *Int. J. Mass Spectrom. Ion Processes* **1999**, 185/186/187, 241.
- (25) Krogh-Jespersen, K. *J. Am. Chem. Soc.* **1991**, 113, 417.
- (26) Schwarz, H. *Int. J. Mass Spectrom.* **2004**, 237, 75.
- (27) Schröder, D.; Schroeter, K.; Zummack, W.; Schwarz, H. *J. Am. Soc. Mass Spectrom.* **1999**, 10, 878 and references therein.
- (28) Roithová, J.; Schröder, D.; Schwarz, H. *J. Phys. Chem. A* **2004**, 108, 5060.
- (29) Vékely, K.; Brenton, A. G.; Beynon, J. H. *J. Phys. Chem.* **1986**, 90, 3569.
- (30) Lammertsma, K.; Schleyer, P. v. R. *J. Am. Chem. Soc.* **1983**, 105, 1049.
- (31) Lias, S. G. Ionization Energy Evaluation. In *NIST Chemistry WebBook, NIST Standard Reference Database Number 69*; Linstrom, P. J., Mallard, W. G., Eds.; National Institute of Standards and Technology: Gaithersburg MD, 20899; March 2003 (<http://webbook.nist.gov>).
- (32) Chase, M. W., Jr. NIST-JANAF Thermochemical Tables, Fourth Edition. *J. Phys. Chem. Ref. Data* **1998**, 9, 1.
- (33) Prosen, E. J.; Gilmont, R.; Rossini, F. D. *J. Res. Natl. Bur. Stand.* **1945**, 34, 65.
- (34) Schröder, D.; Loos, J.; Schwarz, H.; Thissen, R.; Roithová, J.; Herman, Z. *Int. J. Mass Spectrom.* **2003**, 230, 113.
- (35) Steele, W. V.; Chirico, R. D.; Nguyen, A.; Hossenlopp, I. A.; Smith, N. K. *AIChE Symp. Ser.* **1989**, 85, 140.
- (36) Bieri, G.; Burger, F.; Heilbronner, E.; Maier, J. P. *Helv. Chim. Acta* **1977**, 60, 2213.
- (37) Luk'yanova, V. A.; Timofeeva, L. P.; Kozina, M. P.; Kirin, V. N.; Tarakanova, A. V. *Russ. J. Phys. Chem. (Engl. Transl.)* **1991**, 65, 439.
- (38) Only the ionization to the σ -complex of ${}^1\mathbf{3}^{2+}$ is considered. Admittedly, the π -complex of ${}^1\mathbf{3}^{2+}$ lies lower in energy than the σ -complex, but ionization of $\mathbf{3}^{+*}$ to yield π - ${}^1\mathbf{3}^{2+}$ is associated with a larger internal excitation $\Delta E_{v/a} = 0.37$ eV; therefore, the experimental value of the ionization energy most probably corresponds to the formation of a σ -complex.
- (39) Youn, Y. Y.; Choe, J. C.; Kim, M. S. *J. Am. Soc. Mass Spectrom.* **2003**, 14, 110 and references therein.